Glucose Transporter of *Escherichia coli*: NMR Characterization of the Phosphocysteine Form of the IIB^{Glc} Domain and Its Binding Interface with the IIA^{Glc} Subunit†

Gerd Gemmecker,*,‡ Matthias Eberstadt,‡ Andreas Buhr,§,|| Regina Lanz,§ Simona Golic Grdadolnik,‡,⊥ Horst Kessler,‡ and Bernhard Erni§

Institut für Organische Chemie und Biochemie, Technische Universität München, D-85747 Garching, Germany, National Institute of Chemistry, SLO-61115 Ljubljana, Slovenia, and Departement für Chemie und Biochemie, Universität Bern, CH-3012 Bern, Switzerland

Received December 12, 1996; Revised Manuscript Received March 17, 1997⊗

ABSTRACT: The transmembrane subunit of the glucose transporter, IICB^{Glc}, mediates vectorial transport with concomitant phosphorylation of glucose. Glucose phosphorylation proceeds through a cystein phosphate intermediate of the cytosolic IIB domain of IIC^{Glc}, which is phosphorylated by the IIA^{Glc} subunit of the glucose transporter. Two- and three-dimensional NMR experiments were used to characterize the phosphorylation of the 10 kDa subclonal IIB domain and the complementary binding interfaces of [^{15}N]-IIB and [^{15}N]IIA^{Glc}. The largest chemical shift perturbations and the only NOE differences accompanying IIB phosphorylation are confined to the active site residue Cys35, as well as Ile36, Thr37, Arg38, Leu39, and Arg40, which are all located in the turn between strands β1 and β2 and on β2 itself. The significant increase of the amide cross-peak intensities of Ile36, Thr37, and Arg38 upon phosphorylation suggests that the conformational freedom of these groups becomes restrained, possibly due to hydrogen bonding to the oxygens of the bound phosphate and to interactions between the guanidinium group of Arg38 and the phosphoryl group. The residues of IIB which experience chemical shift perturbations upon binding of IIA are located on a protruding surface formed by residues of strands β1, β2, and β4, the β4/α3 loop, and residues from the first two turns of α3. The corresponding binding surface of the IIA^{Glc} domain is comprised of residues on five adjacent β-strands and two short helices surrounding the active site His90. The binding surface of IIA^{Glc} for IIB coincides with the binding surface for HPr, the phosphoryl carrier protein by which IIA^{Glc} is phosphorylated [Chen, Y., Reizer, J., Saier, M. H., Fairbrother, W. J., & Wright, P. E. (1993) *Biochemistry 32*, 32−37].

Protein phosphorylation plays an important role in energy transduction and intracellular signaling, e.g., in the P-type ATPases, protein kinases, and protein phosphatases. The former transport cations across the cell membrane and are transiently phosphorylated on an aspartic acid during turnover (Lutsenko & Kaplan, 1995). The kinases and phosphatases regulate the activity of enzymes and membrane-bound receptors by phosphorylation and dephosphorylation (Bourret et al., 1991; Fantl et al., 1993). In the phosphoenolpyruvate-dependent phosphotransferase system of bacteria (PTS[1]), energy transduction and signaling are two closely intertwined functions. Carbohydrates are accumulated across the cell membrane by a mechanism coupling translocation with phosphorylation of the sugar. Phosphoryl groups are transferred from phosphoenolpyruvate to the transported carbohydrates by a cascade of four phosphohistidine and phosphocysteine protein intermediates (Figure 1). The phosphorylation state of the proteins in the cascade varies with transport activity; i.e., it increases in the absence and decreases in the presence of the corresponding sugar substrate. The ratio of phosphorylated to dephosphorylated proteins in turn serves as signal input for the control of metabolic pathways, of gene transcription, and of chemosensory behavior. The proteins exert their regulatory effect by allosteric interaction with and by phosphorylation of their target proteins [for comprehensive reviews, see Saier (1989), Meadow et al. (1990), Erni (1992), Postma et al. (1993), and Hellingwerf et al. (1995)].

The glucose-specific PTS of *Escherichia coli* is comprised of four subunits: enzyme I, HPr, and the glucose-specific transporter consisting of the soluble subunits IIA^{Glc} and the transmembrane subunit IICB^{Glc} (Figure 1). Enzyme I and HPr are general phosphoryl carrier proteins which deliver phosphoryl groups also to other PTS transporters with

† This study was supported by the Deutsche Forschungsgemeinschaft, the Sonderforschungsbereich 369, the Fond der Chemischen Industrie, the Dr.-Ing. Leonhard Lorenz-Stiftung, and the Swiss National Science Foundation (Grant 31-45838.95). S.G.G. acknowledges support from the Ministry of Science and Technology of Slovenia.

* To whom correspondence should be addressed. Phone: +49 (89) 289-13308. Fax: +49 (89) 289-13210. E-mail: gg@artus.org.chemie.tu-muenchen.de.

‡ Technische Universität München.

§ University of Bern.

|| Present address: Institut für Pharmakologie, Universität Bern, CH-3012 Bern, Switzerland.

⊥ National Institute of Chemistry.

⊗ Abstract published in *Advance ACS Abstracts,* May 15, 1997.

[1] Abbreviations: NMR, nuclear magnetic resonance; PEP, phosphoenolpyruvate; PTS, PEP-dependent sugar phosphotransferase system; IIA^{Glc}, cytoplasmic subunit of the glucose transporter; IICB^{Glc}, transmembrane subunit of the glucose transporter of the PTS; IIB^{Glc}, hydrophilic domain of IICB^{Glc}; IIC^{Glc}, transmembrane domain of IICB^{Glc}; HPr, histidine-containing phosphoryl carrier protein of the PTS; IPTG, isopropyl β-D-thiogalactoside.

S0006-2960(96)03053-X CCC: $14.00

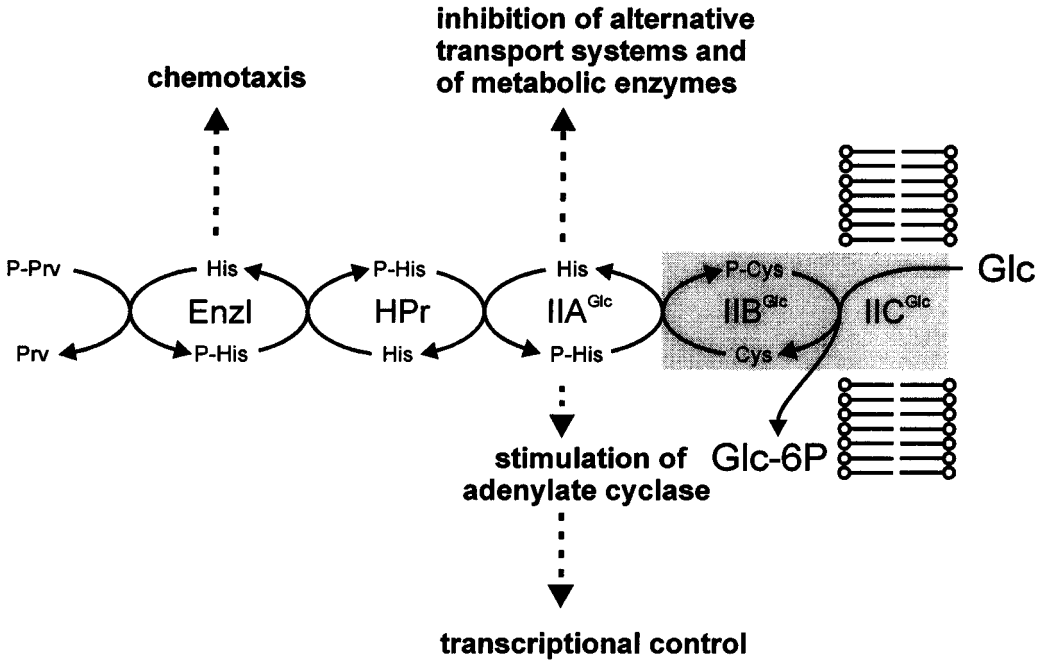

FIGURE 1: Glucose-specific phosphoenolpyruvate-dependent phosphotransferase system. Phosphoryl groups are sequentially transferred from PEP to the transported sugar. The IIB domain of the IICB^{Glc} subunit is phosphorylated at a cysteine; all other proteines are phosphorylated at a histidine side chain. Also indicated are two representative regulatory functions of enzyme I and the IIA^{Glc} subunit (Hurley et al., 1993; Lux et al., 1995).

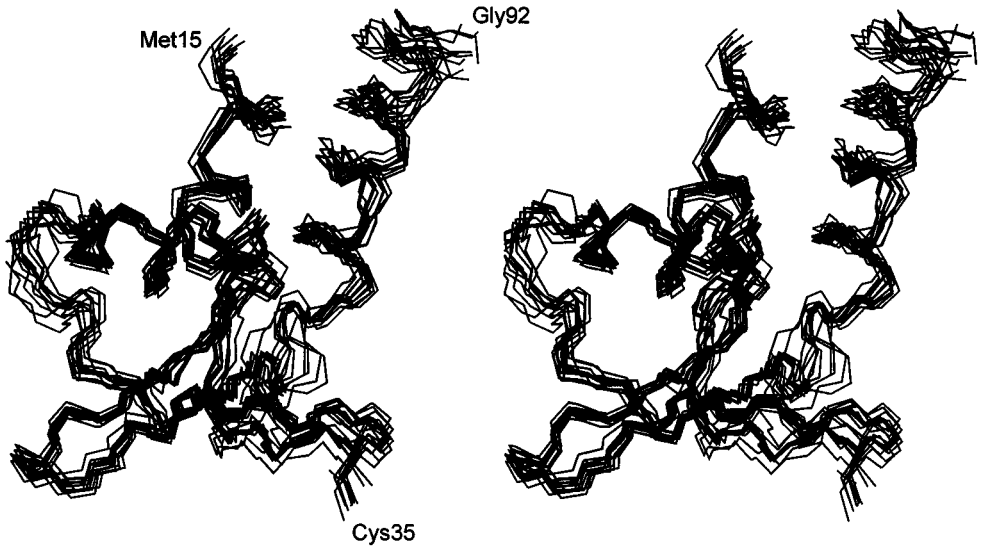

FIGURE 2: Three-dimensional structure of IIB^{Glc} from NMR data (Eberstadt et al., 1996). The representation shows a superposition of the α-carbon traces for residues 15−94 of 11 structures of the IIB^{Glc} domain of *E. coli* (the flexible N and C termini are omitted).

different sugar specificity. There are at least 13 PTS transporters of different but partly overlapping sugar specificity known in *E. coli* which can be grouped into four families according to sequence similarity (Lengeler et al., 1994). The IIA^{Glc} subunit is a β-sheet sandwich with six antiparallel strands on either side, as shown by NMR and X-ray studies with IIA^{Glc} of *E. coli* and the homologous IIA^{Glc} domain of the *Bacillus subtilis* transporter (Fairbrother et al., 1992a,b; Liao et al., 1991; Pelton et al., 1991a,b; Worthylake et al., 1991). IIA^{Glc} of *E. coli* is phosphorylated by HPr at His90, and both the phosphorylated and dephosphorylated forms have been studied by heteronuclear multidimensional NMR (Pelton et al., 1992, 1993). The IICB^{Glc} subunit of the transporter is comprised of two domains, the IIC domain (residues 1−386) spanning the membrane eight times (Buhr & Erni, 1993) and the cytoplasmic IIB domain (residues 387−477) containing the phosphorylation site, Cys421 (Nuoffer et al., 1988; Meins et al., 1993; Buhr et al., 1994). IIC and IIB together catalyze sugar translocation and phosphorylation. The solution structure of the 10 kDa subclonal IIB domain was solved by heteronuclear NMR spectroscopy (Eberstadt et al., 1996). The basic fold consists of a split α/β-sandwich composed of an antiparallel sheet with strand order 1243 and three α-helices superimposed onto one side of the sheet (Figure 2), the sequence of the secondary structure elements being $\alpha\beta\beta\alpha\beta\beta\alpha$. The phosphorylation site Cys35 (corresponding to Cys421 of the whole IICB^{Glc} subunit) is located at the C terminus of β1 on the solvent-exposed face of the β-sheet, surrounded by Thr37 (Thr423 in IICB^{Glc}), Arg38 (Arg424), Arg40 (Arg426), and

Gln70 (Arg456) which are invariant in 15 homologous IIB domains from other PTS transporters (Seqbase release 30.0 EMBL/Swiss-Prot; Sander & Schneider, 1991).

It was shown that phosphoryl transfer occurs not only between IIA and IIB units of the same transporter but also as cross-talk between IIA and IIB units of structurally homologous transporters with different sugar specificity (Vogler et al., 1988; Schnetz et al., 1990), and it has been suggested that the components of the PTS form membrane-associated multiprotein complexes, the actual composition of which might vary, depending on the metabolic requirements of the cell (Scholte et al., 1982; Brouwer et al., 1982; Saier et al., 1982; Misset et al., 1983; Mao et al., 1995b). These observations suggest that one and the same PTS subunit can associate with a number of different proteins from which it accepts and to which it transfers phosphoryl groups in a highly specific way. The modular design with relatively small domains of less than 30 kDa, the variety of their different folds, and the multiple protein interactions involved make the PTS an interesting object for the study of histidine and cysteine phosphorylation and of the specificity of protein−protein contacts. The effect of phosphorylation on the solution structure of the IIB^{Glc} domain and the mapping of the contact regions between IIB^{Glc} and IIA^{Glc} are the subject of this report.

EXPERIMENTAL PROCEDURES

Protein Purification and Sample Preparation. The expression and purification of subclonal ^{15}N- and $^{13}C,^{15}N$-labeled IIB^{Glc} by Ni^{2+} chelate affinity chromatography have been described elsewhere (Buhr et al., 1994; Golic Grdadolnic et al., 1994). For the expression of IIA^{Glc}, the gene *crr* was cloned behind the *Ptac* promoter. The expression plasmid pMScrr1 was constructed by ligating the *Nde*I/*Eco*RI (blunt) insert fragment from plasmid pMacrrN (structural gene for IIA^{Glc}; Schunk, 1992; Mao et al., 1995b) with the *Nde*I/*Hin*dIII (blunt) vector fragment of pMS470Δ8 (expression vector bearing *Ptac* and the *lacI* gene, gift of E. Lanka, Berlin; Fürste et al., 1986). *E. coli* strain W3110(pMScrr1) was grown in 1 L of minimal salts medium supplemented with 1 g of $[^{15}N]NH_4Cl_2$ and 0.6% glucose. When the culture had reached an OD_{550} of 2, protein expression was induced with 0.25 mM IPTG and incubation continued for 10 h. IIA^{Glc} from the cytosolic fraction of 8 g of cells (wet weight) was purified on DEAE-cellulose (7 mL; Mao et al., 1995a); the IIA^{Glc}-containing fractions were concentrated by ultrafiltration (Centriprep-10, Amicon), and IIA^{Glc} was purified by gel filtration (Superdex 75, Pharmacia). Impurities in the shoulder fractions were removed by a second round of gel filtration; the pure peak fractions were pooled, dialyzed against 20 mM NaP_i (pH 6.8), and concentrated by ultrafiltration. The yield was 17 mg of $[^{15}N]IIA^{Glc}$ as determined by quantitative amino acid analysis. NMR spectra were recorded with proteins dissolved in 450 μL of 20 mM NaP_i (pH 6.8), 0.15 M NaCl, 1 mM EDTA, 1 mM NaN_3, 0.5 mM dithiothreitol, 2 mM $MgCl_2$, and 1 mM NaF. D_2O (50 μL) was added for the deuterium lock.

In Situ Phosphorylation of IIB^{Glc}. To continuously regenerate phospho-IIB^{Glc} from hydrolyzed IIB^{Glc}, 20 mM phosphoenolpyruvate, 5 μM enzyme I, 10 μM HPr, and 10 μM IIA^{Glc} were added. No chemical shift changes were observed in the ^{15}N-HSQC spectrum upon addition of phosphoenolpyruvate, $MgCl_2$, and NaF. Addition of catalytic amounts of enzyme I, HPr, and IIA^{Glc} led to phosphorylation of IIB^{Glc} in a few minutes. A series of one-dimensional ^{31}P spectra was recorded over a period of 4 days to monitor the stability of P-IIB^{Glc} (Figure 3). While the intensity of the PEP signal decreased continuously, due to hydrolysis/rephosphorylation of IIB^{Glc}, IIB^{Glc} could be maintained in the phosphorylated state for ca. 100 h.

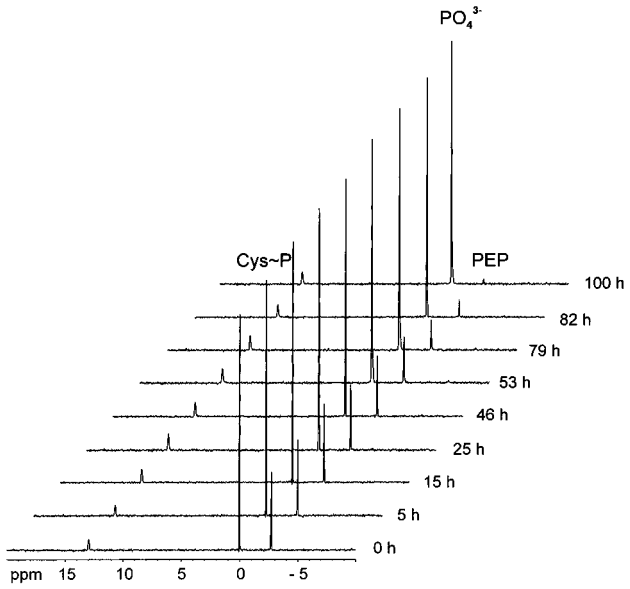

FIGURE 3: Series of ^{31}P spectra of P-IIB^{Glc} recorded after the addition of the phosphorylating enzymes at $t = 0$. The chemical shifts are reported relative to inorganic phosphate at 0 ppm; phosphocystein appears at 11.7 ppm and PEP at −3 ppm. The signal of phosphocystein is unchanged for more than 100 h, while the signal of PEP decreases.

Complexation between IIA^{Glc} and IIB^{Glc}. To examine the interaction between IIA^{Glc} and IIB^{Glc}, mixtures containing 0.5 mM ^{15}N-labeled protein and 1.0 mM unlabeled subunit in a final volume of 0.6 mL were analyzed by heteronuclear NMR. Under these conditions, complexation of the ^{15}N-labeled moiety by the unlabeled protein was complete, as deduced from the $^1H,^{15}N$-correlation spectra.

NMR Spectroscopy. All ^1H-detected NMR spectra were recorded at pH 6.8 and 300 K on a Bruker AMX600 spectrometer equipped with shielded z-gradients (ca. 50 G/cm). The one-dimensional ^{31}P spectra shown in Figure 3 were measured on a Bruker AMX500 spectrometer.

The two-dimensional ^{15}N-HSQC spectra (Bax et al., 1990) of IIB^{Glc}, P-IIB^{Glc}, and the IIA^{Glc}/IIB^{Glc} complexes, as well as the three-dimensional ^{15}N-TOCSY−HSQC experiment (Marion et al., 1989a; with a 50 ms DIPSI-2 mixing period, Shaka et al., 1988) and the three-dimensional ^{15}N-NOESY−HSQC spectrum (Marion et al., 1989b; Kay et al., 1989; with 50 ms NOE mixing time) of P-IIB^{Glc}, were recorded and processed as described (Golic Grdadolnik et al., 1994).

Assignment of the residues was achieved by comparison with the published chemical shifts and connectivities of unphosphorylated IIA^{Glc} (Pelton et al., 1991a,b) and IIB^{Glc} (Golic Grdadolnik et al., 1994; Eberstadt et al., 1996) and from evaluation of the NOESY and TOCSY correlation data for phospho-IIB^{Glc}.

The three-dimensional surfaces (Figures 7, 9, and 11) were generated by the MOLCAD module of SYBYL (Tripos AG, Version 6.2) from calculated electron densities.

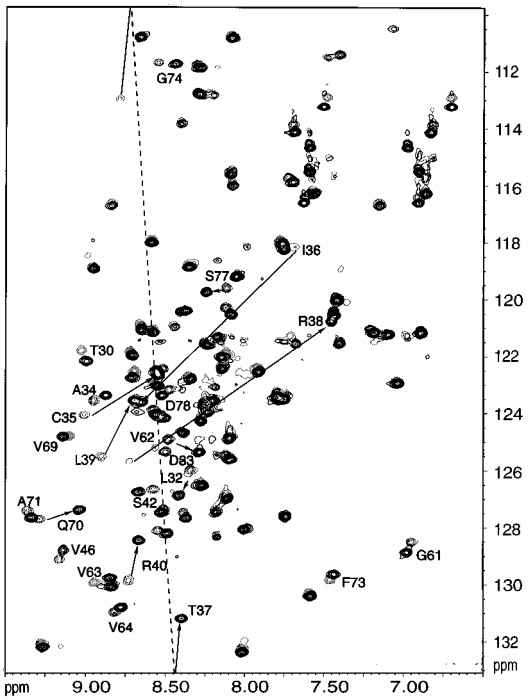

FIGURE 4: Overlay of the ^{15}N-HSQC spectra of the unphosphorylated (gray contours) and phosphorylated (black contours) IIB^{Glc} domain of *E. coli* at 300 K and pH 6.8. Signals that show a significant shift upon phosphorylation are labeled with their residue type and sequential position (the signal of Thr37 is folded, as indicated by the broken arrow).

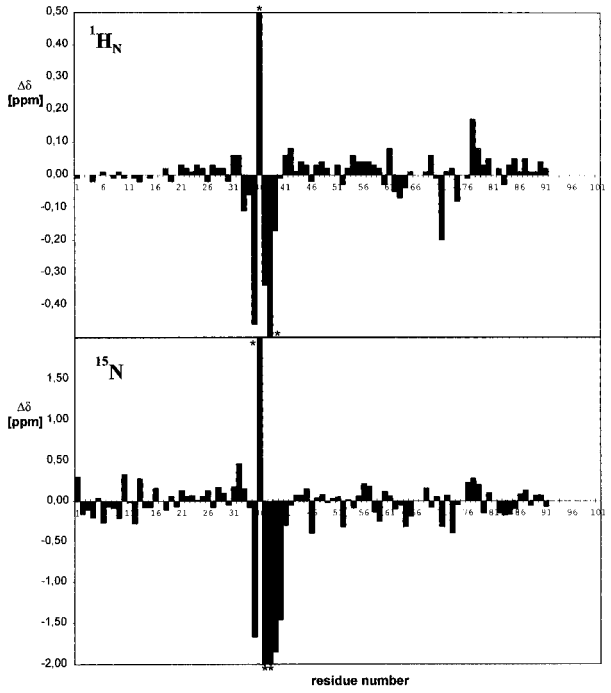

FIGURE 5: Chemical shift differences for $^{1}H_N$ and ^{15}N of the backbone amide signals of IIB^{Glc} phosphorylated at Cys35, relative to unphosphorylated IIB^{Glc}. In addition to Pro17, the amide signals of residues Asn4, Gly66, Ser67, and Thr75 could not be detected; their chemical shift differences were therefore set to zero.

RESULTS

Cysteine Phosphorylation. The thiophosphate ester of phospho-IIB^{Glc} has a half-life of 40 h (Buhr et al., 1994). To regenerate P-IIB^{Glc}, PEP and catalytic amounts of enzyme I, HPr, and IIA^{Glc} were added. The addition of PEP alone does not have an effect on the NMR spectrum of IIB^{Glc} (not shown). Only when the phosphoryl carrier proteins enzyme I, HPr and IIA^{Glc} were also included did a ^{31}P signal appear at 11.7 ppm, which is characteristic of phosphate thioesters (Pas et al., 1991; Robillard et al., 1993). The chemical shift as well as the intensity of the signal remains unchanged for over 100 h, while the ^{31}P resonance of PEP at −3 ppm decreases continuously due to hydrolysis of the phosphate thioester and ensuing consumption of PEP (Figure 3). This *in situ* regeneration system allowed the acquisition of a two-dimensional ^{15}N-HSQC spectrum and of two heteronuclear three-dimensional NMR experiments (three-dimensional HSQC-TOCSY and three-dimensional HSQC-NOESY) of phosphorylated IIB^{Glc}.

Structural Changes Induced by Phosphorylation. The effect of phosphorylation of IIB^{Glc} can be followed by an analysis of the ^{15}N-HSQC spectrum shown in Figure 4, with the signals in gray being ^{1}H−^{15}N correlations of the unphosphorylated protein and the signals in black showing ^{1}H−^{15}N correlations of the phosphorylated IIB^{Glc} domain. Obviously, most resonances do not change their position in the spectrum upon phosphorylation. However, some resonances exhibit significant shifts after addition of the PTS components and PEP. In particular, the amide signals of the residues clustered around the active site (residues 34−40) change their position in the ^{15}N-HSQC spectrum considerably.

Assignment of the signals of phosphorylated IIB^{Glc} could often be accomplished by a simple comparison of the spectra before and after phosphorylation. This procedure worked well for the majority of only slightly shifted amide signals. Only those amide resonances experiencing large chemical shift changes (residues Cys35, Ile36, Thr37, Arg38, Leu39, and Arg40) had to be assigned using three-dimensional ^{15}N-TOCSY−HSQC and three-dimensional ^{15}N-NOESY−HSQC spectra. Furthermore, assignments of several side chain ^{1}H resonances of P-IIB^{Glc} were obtained from the three-dimensional TOCSY−HSQC spectrum. Many of the H$^{\alpha}$ and H$^{\beta}$ protons as well as the methyl groups of alanine, valine, isoleucine, and leucine could thus be identified. However, some of the lysine and arginine side chain protons could not be assigned unambiguously due to spectral overlap in these regions.

A quantitative summary of the observed amide chemical shift changes (represented as the difference between the chemical shifts of the amide resonances in the dephosphorylated and phosphorylated state) reveals that the largest chemical shift changes occur for the conserved residues around the active site, i.e., Leu32−Arg40 (Figure 5). There are also smaller but still significant changes in chemical shifts occurring in residues Thr30, Ser42, Val46, Gly61, Val62, Val63, Val64, Val69, Gln70, Ala71, Phe73, Gly74, Ser77, and Asp78.

However, quantitative results of structural changes upon protein phosphorylation should not be deduced from chemical shift changes alone. Detailed information about the three-dimensional structure of a molecule is best obtained from NOEs, reflecting proton−proton distances in the three-dimensional structure. Therefore, three-dimensional ^{15}N-edited NOESY spectra in the dephosphorylated state were compared with the same spectra of the protein in the phosphorylated form. In Figure 6, strips from the three-dimensional ^{15}N-NOESY−HSQC spectra in both states are aligned for the residues around the active site experiencing

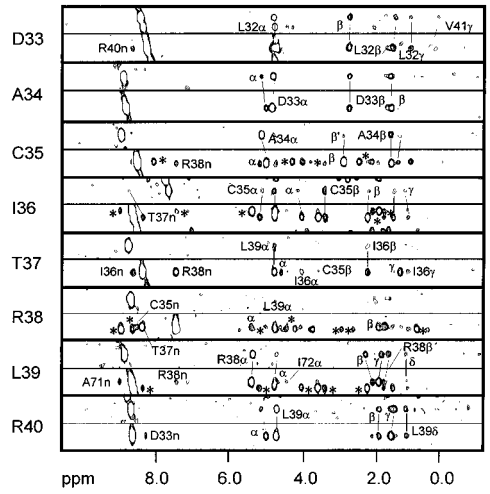

FIGURE 6: Strips taken from the three-dimensional ^{15}N-NOESY−HSQC spectrum of IIB^{Glc} (top slice) and P-IIB^{Glc} (bottom slice) for residues clustered around the active site and whose amide signals exhibit significant chemical shift changes. Lines correlate NOEs between identical proton pairs; intraresidual NOEs are indicated by the Greek letters denoting their position, without residue labels. The NOE patterns of Cys35, Ile36, Thr37, Arg38, and Leu39 are complicated in the spectrum of P-IIB^{Glc} by overlap of their amide signals with other amide signals in both the proton and nitrogen dimensions (marked with an asterisk).

the largest changes of amide chemical shifts. Other residues with no or only small chemical shift changes show practically identical NOESY spectra in the phosphorylated and dephosphorylated state.

For some residues, this comparison was complicated by overlapping amide signals; the ^{1}H−^{15}N correlations of residues Cys35, Ile36, Arg38, and Leu39 are obscured by the amide signals of residues Asp85, Leu39, Asn31, and Ile36, respectively, in the phosphorylated state, though not in the unphosphorylated protein (cf. Figure 4). However, a detailed inspection of the three-dimensional NOESY spectrum shows that only very few *new* NOE cross-peaks emerge in the spectrum of the phosphorylated protein; the amide protons of residues Ile36, Thr37, Arg38, and Leu39 exhibit more NOE correlations after phosphorylation, especially the H^N−H^N NOEs of Thr37 with Ile36 and Arg38 become very intense (cf. Table 1). The few new NOEs in the phosphorylated protein are only found between protons that are already close neighbors in the unphosphorylated structure. Therefore, significant changes of the conformation of IIB^{Glc} upon phosphorylation can be excluded, except for minor rearrangements at the phosphorylation site. Thus, using the three-dimensional structure of the *unphosphorylated* IIB^{Glc} for a visual representation of observed amide shifts in the *phosphorylated* protein is justified (Figure 7); the affected residues are all clustered in spatial proximity to the active site Cys35, either in strands 1, 2, and 4 of the β-sheet or in the loop region connecting β4 to the C-terminal helix α3.

The amide protons of Ile36, Thr37, and Arg38 in the loop region between β1 and β2 show extreme exchange broadening in the unphosphorylated state, leading to very low intensity in the ^{15}N-HSQC spectrum (see Figure 3, gray signals of Ile36, Thr37, and Arg38). In the phosphorylated state, however, these signals are as sharp and intense as the other amide signals in the ^{15}N-HSQC spectrum (see Figure 3, black signals of Ile36, Thr37, and Arg38). This effect might contribute to the already mentioned increase in NOEs

Table 1: Observed NOE Intensity Changes in the Three-Dimensional ^{15}N-NOESY−HSQC Spectrum of P-IIB^{Glc} vs IIB^{Glc}

residues	P-IIB^{Glc}	IIB^{Glc}
D33H^N−R40H^N	medium	missing
D33H^N−I32H$^\beta$	weak	missing
C35H^N−R38H^N	medium	weak
C35H^N−C35H$^\alpha$	medium	missing
C35H^N−C35H$^\beta$	very weak	missing
C35H^N−C35H$^{\beta'}$	strong	weak
I36H^N−T37H^N	medium	very weak
T37H^N−R38H^N	strong	missing
T37H^N−T37H$^\alpha$	medium	missing
T37H^N−I36H$^\alpha$	weak	missing
T37H^N−C35H$^\beta$	very weak	missing
T37H^N−I36H$^\beta$	strong	weak
T37H^N−T37H$^\gamma$	strong	missing
T37H^N−I36H$^\gamma$	weak	missing
R38H^N−R38H$^\alpha$	medium	missing
R38H^N−L39H$^\alpha$	strong	missing
R38H^N−R38H$^\beta$	medium	missing
L39H^N−A71H^N	weak	very weak
L39H^N−R38H^N	weak	missing
L39H^N−I72H$^\alpha$	very weak	missing

observed for these amide signals in the phosphorylated state. The significant line sharpening is a clear indication of a stiffening of the three-dimensional structure in this region upon phosphorylation, probably caused by the formation of hydrogen bonds with oxygen atoms of the phosphoryl group at Cys35.

Interaction between IIA^{Glc} and IIB^{Glc}. Phosphoryl transfer from IIA^{Glc} to IIB^{Glc} proceeds by an in-line associative mechanism resulting in inversion of configuration at the phosphorus atom (Begley et al., 1982). His90 of IIA^{Glc} and Cys35 of IIB^{Glc} become transiently bridged by the phosphoryl group in this process. The investigation of the complexation of both proteins followed a course similar to that of the phosphorylation experiments. ^{15}N-HSQC spectra of the uncomplexed forms of both proteins IIA^{Glc} and IIB^{Glc} were compared to the ^{15}N-HSQC spectra of the complexed ones (not shown). Due to the larger size of the IIA/IIB complex (ca. 26 kDa) and the lower concentration (ca. 0.5 mM) of the observable ^{15}N-labeled moiety, when compared to the phosphorylated IIB^{Glc} sample, the acquisition of three-dimensional ^{15}N-edited spectra was not feasible any more. Nevertheless, assignment and determination of the chemical shift differences between the complexed and free state were still possible for the majority of the IIA^{Glc} as well as the IIB^{Glc} amide signals (cf. Figures 8 and 10). Again, a change of the chemical shifts of the amide signals can be related to an interaction of a particular residue with the complex partner. Significant shifts upon complex formation were observed for the following amide signals of IIA^{Glc}: I23, V31, N32, I33, N36, V40, F41, A42, E43, I45, D48, G49, I50, I52, G56, T66, I67, G68, K69, I70, F71, E72, T73, N74, H75, A76, F77, S78, I79, E80, D82, E86, L87, F88, V89, H90, F91, I93, D94, T95, V96, K99, G100, E101, G110, Q111, K132, S133, T134, V138, V139, I140, S141, N142, M143, D144, I150, and I166 (Figure 8). In IIB^{Glc}, complexation caused significant amide shifts in residues V20, T30, L32, D33, A34, C35, I36, T37, R38, L39, R40, V41, S42, A60, G61, V63, G68, V69, A71, I72, F73, G74, K76, D78, L80, E83, D85, and I88 (Figure 10). Figures 9 and 11 depict the observed effects on the three-dimensional structures of IIA^{Glc} and IIB^{Glc}; residues with significantly shifted

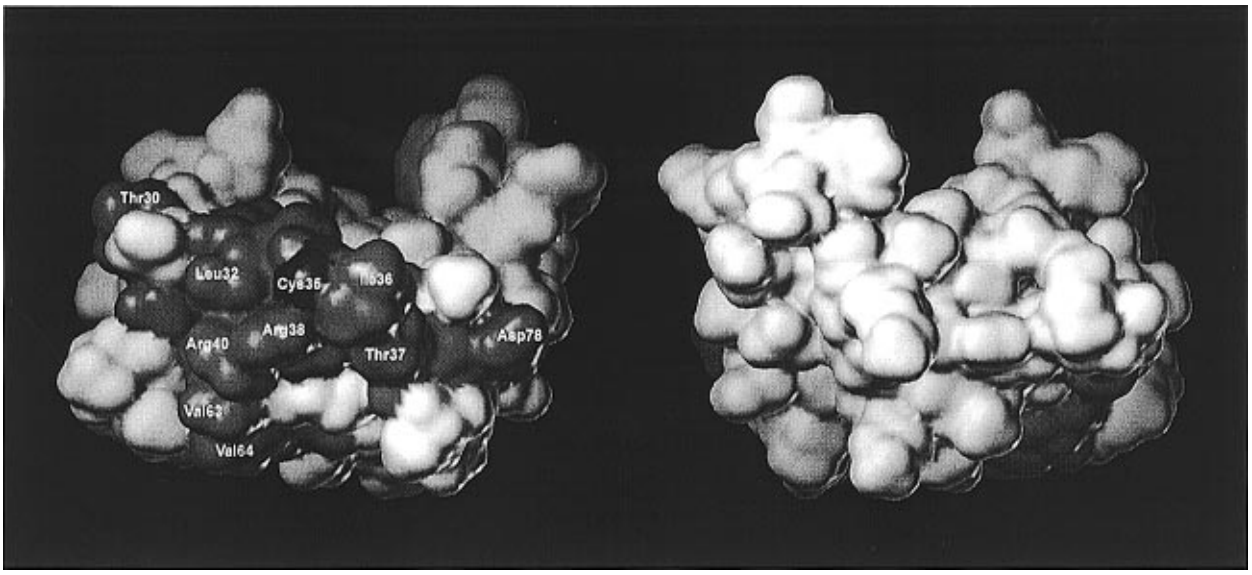

FIGURE 7: Effects of phosphorylation of IIB^{Glc} at Cys35 (phosphate group not shown), displayed on the three-dimensional structure of the protein (Eberstadt et al., 1996; Brookhaven Protein Data Bank ID code 1iba). Residues experiencing a significant amide shift upon phosphorylation are shown with shading on the electron density surface. Several residue labels are provided for orientation: (left) a view of the active site Cys35 and (right) a view from behind (after a 180° rotation about a vertical axis through the center of the molecule). Obviously, the observed effects are limited to the spatial neighborhood af the phosphorylation site.

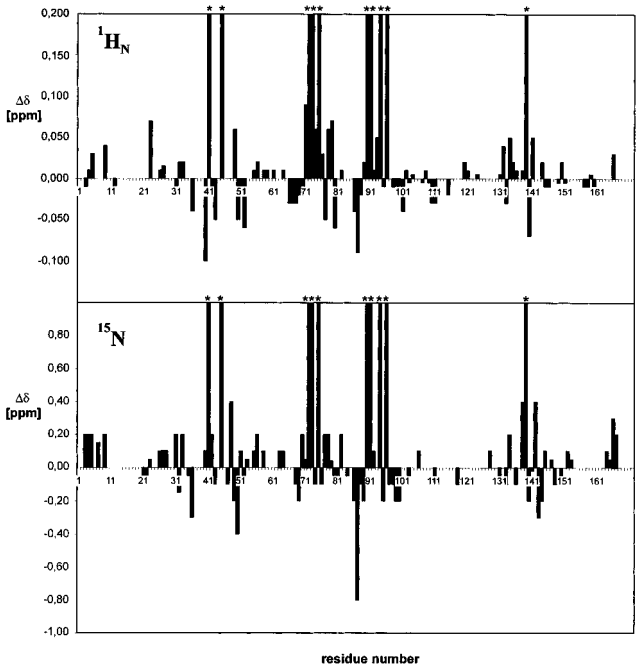

FIGURE 8: Chemical shift differences for ^1H_N and ^{15}N of the backbone amide signals of residues 1−168 of IIA^{Glc} complexed with IIB^{Glc}. In addition to the proline residues at positions 25, 37, 54, 62, 125, 137, and 162, the amide signals of some residues could not be observed (G1, L2, S8, V10, V46, N57, and S83) or assigned unambiguously due to overlap in the ^{15}N-HSQC spectra (L6, D13, T19, E29, D38, V39, K44, V85, D117, D123, L127, K130, and K167). For residues F41, I45, E72, T73, H75, H90, F91, D94, V96, and V139, no unambiguous assignment was possible for the complexed state, but the chemical shift differences clearly exceed 1 ppm for both ^1H_N and ^{15}N (marked with an asterisk).

amide signals as well as the active site residues (His75 and His90 of IIA^{Glc} and Cys35 of IIB^{Glc}) are indicated by dark shading.

As expected, residues of IIA^{Glc} surrounding the active site His75 and His90 show the largest chemical shift changes (Figures 8 and 9, left panel). IIA^{Glc} is a sandwich of two β-sheets, each consisting of six antiparallel strands. The observed chemical shift changes are clustered on five strands of the sheet containing the active site (D48, G49, I50, and I52; I70 and F71; H75, A76, F77, S78, I79, and E80; E86, L87, F88, V89, H90, F91, and I93; V138, V139, I140, and S141), in the two short helices adjacent to the active site (I33 and N36; V40, A42, and E43; D94, T95, V96, and K99), and in nonperiodic structures of the same face (I45, K69, I70, F71, T73, N74, S133, T134, N142, and M143). Only one residue showing small chemical shift changes is located on the rear face of the protein (I23, Figure 9, right panel).

The residues of IIB^{Glc} experiencing the biggest shift changes are located close to the active site Cys35 (Figures 10 and 11, left panel), namely in the first two strands of the β-sheet (T30, L32, D33, A34, C35, I36, T37, R38, L39, R40, V41, and S42), in the loops after α-helix 2 (A60 and G61) and β-strand 4 (A71, I72, F73, and G74), and in α-helix 3 (K76, D78, L80, E83, and D85). No significant shifts were observed for any of the residues on the opposite side of IIB^{Glc} (Figure 11, right panel).

DISCUSSION

The IIB^{Glc} domain of the glucose transporter has two functions. On one hand, it transfers a phosphoryl group from IIA^{Glc} to the sugar substrate, on the other hand, it is necessary for sugar translocation by the IIC domain. Neither the IIC domain alone nor unphosphorylated IICB^{Glc} or a IICB^{Glc} mutant with a glutamic acid in place of the active site cysteine is capable of sugar transport (Buhr et al., 1994; A. Buhr and Q. Mao, unpublished results). Two arginines of the IICB^{Glc} subunit (Arg426 and Arg428, corresponding to Arg38 and Arg40 of the subclonal IIB domain) are essential for transport and phosphorylation of glucose but not for phosphorylation of IICB^{Glc} by the IIA^{Glc} subunit (R. Lanz and B. Erni, unpublished mutagenesis results).

Protein phosphorylation can induce local or global conformational changes in the phosphorylated structure itself and affect the structure of and association to other protein subunits, mainly by electrostatic interactions (Johnson &

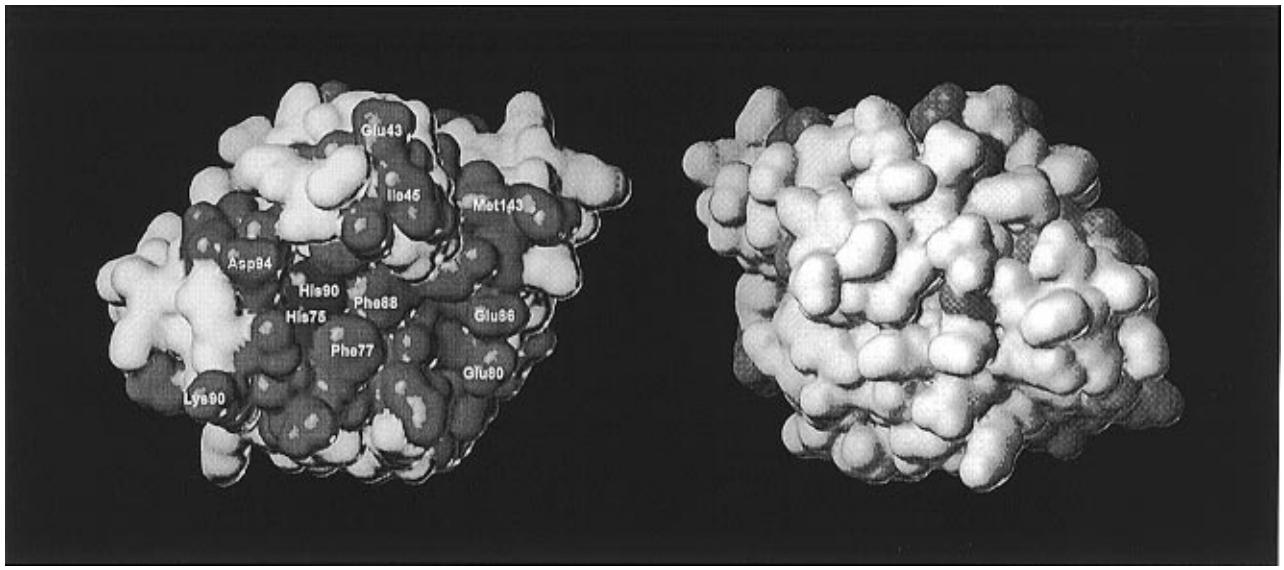

FIGURE 9: Electron density surface of IIA^{Glc} of *E. coli*, calculated from the X-ray structure (Worthylake et al., 1991; Brookhaven Protein Data Bank ID code 1f3g). Backbone atoms of residues with significant (i.e., >12 Hz) amide signal shifts upon binding to IIB^{Glc} are shown with dark shading, as well as the active site residues His75 and His90: (left) a view of the postulated binding site with the active site in its center, with several residues having labels for easy orientation, and (right) a view from the opposite direction (rotated by 180° about a vertical axis relative to the left panel).

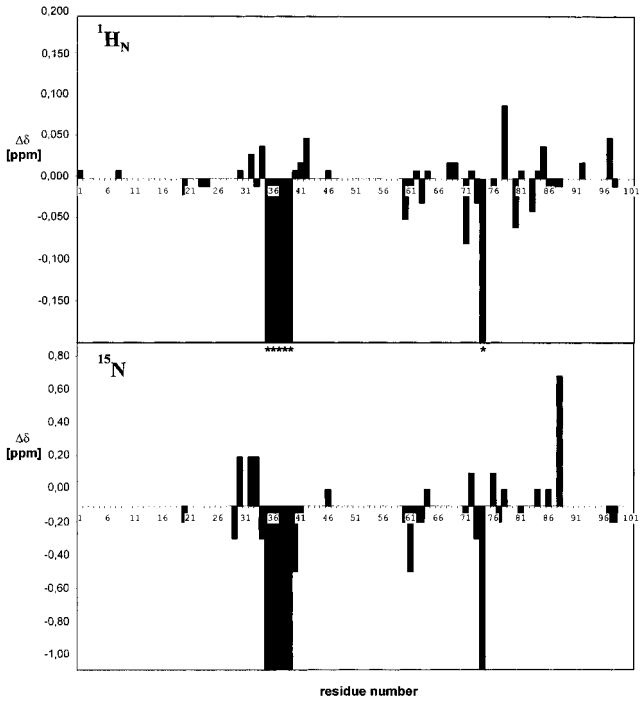

FIGURE 10: Chemical shift differences for ^1H_N and ^{15}N of the backbone amide signals of IIB^{Glc} complexed with IIA^{Glc}, relative to free IIB^{Glc}. The chemical shift differences of residues Cys35, Ile36, Thr37, Arg38, Leu39, and Gly74 (marked with an asterisk) could not be determined unambiguously; however, they exceed 1 ppm for ^1H_N and ^{15}N. The values for Pro17 and Thr75 (missing assignment in free IIB^{Glc}) were set to zero.

Barford, 1993). Phosphorylation of the IIB domain could trigger a conformational transition of the IIC^{Glc} and/or the IIB^{Glc} domain and thus affect the vectorial translocation of the substrate.

Protein Phosphorylation. The NMR chemical shift is a sensitive parameter for changes in the local nuclear environment in molecules, i.e., the surrounding electron density (affected by electrostatic effects of neighboring nuclei, hydrogen bonding, etc.), peptide bond anisotropy, aromatic ring current effects, and more. Chemical modifications of and complex formation between macromolecules will generally cause chemical shift perturbations at the corresponding interaction sites, via either local conformational changes or any other effects on the local electron distribution (Wittekind et al., 1990). A qualitative evaluation of chemical shift changes can therefore be used for the detection and localization of effects caused by protein phosphorylation or the formation of a protein/protein complex (Pelton et al., 1992).

Chemical shift perturbations were used to analyze the structural changes of the IIB domain of the glucose transporter upon phosphorylation. A comparison of the ^{15}N-HSQC spectra of the phosphorylated and unphosphorylated protein shows that the majority of the ^1H_N and ^{15}N signals do not shift upon phosphorylation; therefore, it can be concluded that IIB^{Glc} does not undergo a global structural change after phosphorylation at Cys35. The majority of the residues affected by phosphorylation are located in the turn between the first and second β-strands immediately adjacent to the active site. The size of the chemical shift changes observed for these residues (up to ca. ±1 ppm for $^1H^N$ and ±5 ppm for ^{15}N) is comparable to that of the changes reported for the immediate environment of a phosphorylation site (Pelton et al., 1992). The close correspondence between NOE cross-peak patterns in the two three-dimensional ^{15}N-NOESY−HSQC spectra indicates that larger conformational changes do not occur at the active site either (cf. Figure 6 and Table 1). Differences in cross-peak intensities and a few new intraresidual and sequential NOEs for the amide protons of Cys35, Ile36, Thr37, and Arg38 point to the possibility of small conformational changes in this region. Most conspicuous is the strong intensity difference of the amide signals of residues Ile36−Leu39 in the ^{15}N-HSQC spectrum, indicating that the fast exchange of the amide protons at the active site of IIB^{Glc} slows upon phosphorylation. This effect can be explained by hydrogen bonding between the backbone amide protons of the active site residues and oxygens of the bound phosphate, as well as by

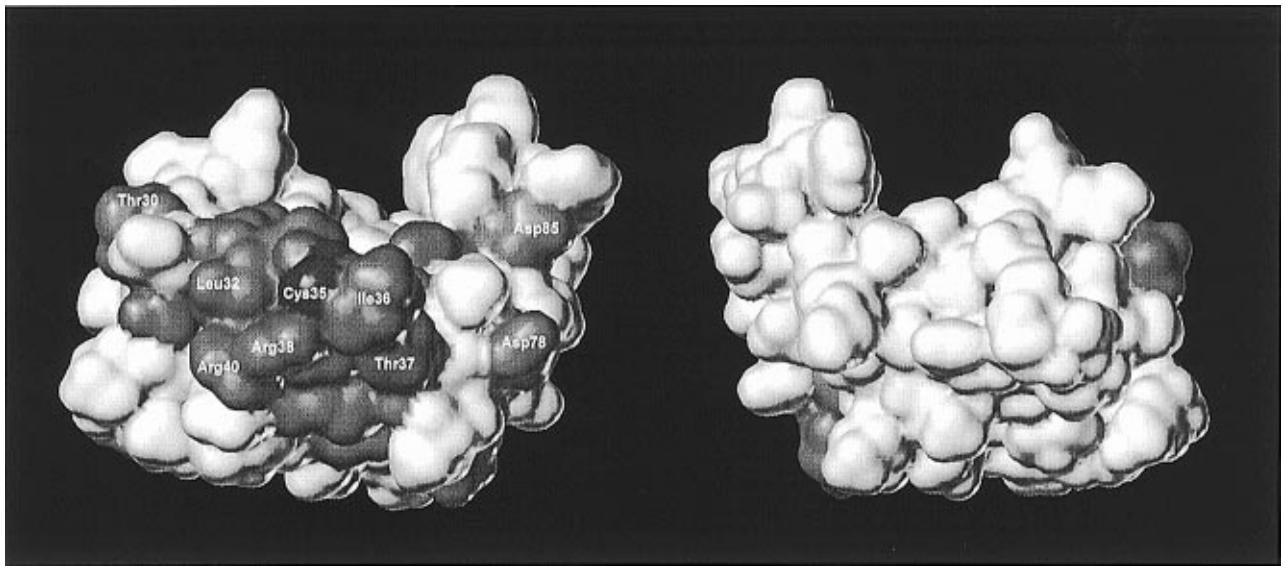

FIGURE 11: Electron density surface of IIB^{Glc} of *E. coli*, calculated from the solution NMR structure (Eberstadt et al., 1996; Brookhaven Protein Data Bank ID code 1iba). Similar to Figure 7, backbone atoms of residues exhibiting significant amide signal shifts (>12 Hz) upon binding to IIA^{Glc} are shown with dark shading, as well as the phosphorylation site residue Cys35: (left) a view of the postulated binding site, which is again centered around the active site (residue labels are provided for orientation only), and (right) a view from the opposite direction (rotated by 180° about a vertical axis relative to the left panel).

electrostatic and hydrogen bonding interactions of the phosphate group with the side chain of Arg38.

There are two groups of phosphoproteins which are of particular interest for comparison. The first group comprises the phosphotyrosine phosphatases (PTPases), the only proteins with cysteine-containing phosphorylation sites for which high-resolution X-ray structures are known (Stuckey et al., 1994; Su et al., 1994; Barford et al., 1994; Fauman & Saper, 1996). Comparison of the native and tungstate complexed structures of the high-molecular mass PTPases showed that only localized protein conformation changes accompany tungstate binding and that the tungstate oxygens in the active site undergo hydrogen bonding to the main chain nitrogen atoms of the active site loop. The active site sequences HCXAGXRS/T and CLGNICR of the high- and low-molecular mass PTPases, resepectively, contain arginines five to six residues downstream from Cys, a feature which is shared by the invariant CXTRLR sequences of the homologous IIB domains. For the PTPases, it was demonstrated that the side chain of arginine encircles the tungstate ion (Barford et al., 1994; Stuckey et al., 1994).

The phosphoryl carrier protein HPr, the IIA^{Glc} subunit, the subclonal IIA domain of the mannitol transporter (IICBA^{Mtl}) of the bacterial phosphotransferase system, and the chemotaxis kinase CheA comprise the second group of interest. However, these proteins are phosphorylated at a histidine rather than at a cysteine. The effects of phosphorylation have been investigated by high-resolution NMR and X-ray techniques (Jia et al., 1993; Pelton et al., 1992, 1993; van Nuland et al., 1993, 1994, 1995, 1996; Rajagopal et al., 1994; Zhou et al., 1995). Chemical shift changes observed upon phosphorylation of these proteins are restricted to the surroundings of the active site. The phosphoryl group bound to His15 of HPr is most likely complexed by the guanidino group of Arg17, as inferred from the observed restriction of the latter's conformational freedom and from ^{31}P chemical shift changes (Rajagopal et al., 1994). However, more recently, this stabilization of the phosphoryl group by Arg17 has been questioned, on the basis of a molecular dynamics simulation of phospho-HPr in water (van Nuland et al., 1995, 1996). It has been postulated that in the IIA^{Glc}/HPr complex the Arg17 side chain of HPr switches between the phosphoryl group at His15 of HPr and the carboxylic groups of Asp31 and Asp87 of IIA^{Glc} (Herzberg, 1992). As the active sites of HPr and IIB^{Glc} interact with the same phosphorylation site on IIA^{Glc}, Arg38 or Arg40 of the IIB domain may function similarly (see below).

Protein−Protein Interactions. The IIB^{Glc} domain is phosphorylated by the IIA^{Glc} subunit of the glucose transporter. This necessitates specific interactions between the two proteins. Chemical shift changes are indicative of a specific interaction between proteins and can be used to map the binding surfaces (Takahashi et al., 1991). For the exact determination of the relative orientation of the two subunits in the complex, a set of intermolecular NOEs would be required, yielding specific distance constraints between the residue pairs involved. Such NOEs could not be detected in our ^{15}N-labeled complexes, which is not surprising, since most protein−protein contacts will arise between the side chains and are not accessible from ^{15}N-edited spectra. However, some information about the complex can be deduced from combining NMR spectroscopic and biochemical data. So the amide resonances that shift upon binding between IIB^{Glc} and the IIA^{Glc} subunit belong to residues located on a continuous surface around the two phosphorylation sites (His90 and Cys35). Since the perturbations are restricted to a small area of the protein surface, a change of the overall conformation upon complex formation is unlikely. The binding surfaces of IIB^{Glc} and IIA^{Glc} appear to be complementary in shape and chemistry. While the phosphorylation site of IIA^{Glc} is situated in a concave hydrophobic depression (Herzberg, 1992; Worthylake et al., 1991), the active site cysteine of IIB^{Glc} is located on a hydrophobic protrusion (Eberstadt et al., 1996). Most of the residues in the contact area have nonpolar side chains; therefore, hydrophobic interactions may play a predominant role.

When S of Cys35 and N3 of His90 are brought into the apical positions of a bridging (trigonal bipyramidal) phosphorus and the binding surfaces (as derived from the chemical shift perturbations) are aligned, an arrangement with the β-sheets of IIB^{Glc} and IIA^{Glc} oriented parallel to each other appears to be most plausible. Located in the mainly hydrophobic contact area of IIA^{Glc} are the strongly conserved polar residues Ser141 (Ser or Thr in all 18 homologous IIA domains), Glu86 (Glu or Asp in 16 out of 18 IIA domains), and Lys69 (invariant in all IIA domains from Gram-negative bacteria). Gln70 is invariant in the contact area of IIB. These residues could further specify the relative orientation and the interactions by participating in hydrogen bonds between IIA^{Glc} and IIB^{Glc}.

IIA^{Glc} which donates its phosphoryl group to IIB^{Glc} is itself phosphorylated by the 9 kDa phosphoryl carrier protein HPr. It is therefore likely that the contact surfaces of IIA^{Glc} for HPr and IIB^{Glc} are overlapping. The binding interfaces of IIA^{Glc} and HPr of *B. subtilis* (which are very similar to the respective *E. coli* proteins) have been mapped by NMR experiments (Chen et al., 1993), and an atomic model for the complex between HPr and IIA^{Glc} has been proposed on the basis of energy minimization of the docked high-resolution X-ray structures (Herzberg, 1992). The binding surfaces for HPr and IIB^{Glc} are similar as both are located on the five β-strands and two α-helices surrounding the active site of IIA^{Glc}. In contrast, the contact and active site areas of IIB^{Glc} and HPr are different. HPr and IIB^{Glc} are both split α/β-sandwiches of three α-helices and an antiparallel β-sheet (IIB^{Glc}, $\alpha\beta\beta\alpha\beta\beta\alpha$, strand order 1243; HPr, $\beta\alpha\beta\beta\alpha\beta\alpha$, strand order 1423). However, IIB^{Glc} contacts IIA through the β-sheet, while HPr mainly binds through α-helix 1; the active site of IIB^{Glc} is located on a turn between strands $\beta1$ and $\beta2$, while in HPr, its position is in the loop between $\beta1$ and $\alpha1$.

The effect of phosphorylation on the IIB^{Glc} domain is similar to that found for the other PTS proteins HPr and IIA^{Glc}. The phosphoryl group obviously has only little influence on the global fold of these three proteins, which is not unexpected, since the phosphorylation site is located on the surface of the protein and exposed to the solvent. The small phosphoryl group can be added to the cysteine or histidine side chain without a need for structural rearrangement. However, while HPr and IIA^{Glc} serve, at least in a first approximation, only as phosphoryl transfer catalysts, the IIB^{Glc} domain is expected to be involved also with the IIC-dependent vectorial transport of glucose. How IIB and IIC are conformationally coupled and what role phosphorylation plays in this process remain open questions for the moment.

REFERENCES

Barford, D., Flint, A. J., & Tonks, N. K. (1994) *Science 263*, 1397−1404.

Bax, A., Ikura, M., Kay, L. E., Torchia, D. A., & Tschudin, R. (1990) *J. Magn. Reson. 86*, 304−318.

Begley, G. S., Hansen, D. E., Jacobson, G. R., & Knowles, J. R. (1982) *Biochemistry 21*, 5552−5556.

Bourret, R. B., Borkovich, K. A., & Simon, M. I. (1991) *Annu. Rev. Biochem. 60*, 401−441.

Brouwer, M., Elferink, M. G. L., & Robillard, G. T. (1982) *Biochemistry 21*, 82−88.

Buhr, A., & Erni, B. (1993) *J. Biol. Chem. 268*, 11599−11603.

Buhr, A., Flükiger, K., & Erni, B. (1994) *J. Biol. Chem. 269*, 23437−23443.

Chen, Y., Reizer, J., Saier, M. H., Fairbrother, W. J., & Wright, P. E. (1993) *Biochemistry 32*, 32−37.

Eberstadt, M., Golic Grdadolnik, S., Gemmecker, G., Kessler, H., Buhr, A., & Erni, B. (1996) *Biochemistry 35*, 11286−11292.

Erni, B. (1992) *Int. Rev. Cytol. 137A*, 127−148.

Fairbrother, W. J., Palmer, A. G., III, Rance, M., Reizer, J., Saier, H. M., & Wright, P. E. (1992a) *Biochemistry 31*, 4413−4425.

Fairbrother, W. J., Gippert, G. P., Reizer, J., Saier, H. M., Jr., & Wright, P. E. (1992b) *FEBS Lett. 296*, 148−152.

Fantl, W. J., Johnson, D. E., & Williams, L. T. (1993) *Annu. Rev. Biochem. 62*, 453−481.

Fürste, J. P., Pansegrau, W., Frank, R., Blöcker, H., Scholz, P., Bagdasarian, M., & Lanka, E. (1986) *Gene 48*, 119−131.

Golic Grdadolnik, S., Eberstadt, M., Gemmecker, G., Kessler, H., Buhr, A., & Erni, B. (1994) *Eur. J. Biochem. 219*, 945−952.

Hellingwerf, K. J., Postma, P. W., Tommassen, J., & Westerhoff, H. V. (1995) *FEMS Microbiol. Rev. 16*, 309−321.

Herzberg, O. (1992) *J. Biol. Chem. 267*, 24819−24823.

Hurley, J. H., Faber, H. R., Worthylake, D., Meadow, N. D., Roseman, S., Pettigrew, D. W., & Remington, S. J. (1993) *Science 259*, 673−677.

Jia, Z., Vandonselaar, M., Quail, J. W., & Delbaere, L. T. J. (1993) *Nature 361*, 94−97.

Johnson, L. N., & Barford, D. (1993) *Annu. Rev. Biophys. Biomol. Struct. 22*, 199−232.

Kay, L. E., Marion, D., & Bax, A. (1989) *J. Magn. Reson. 84*, 72−84.

Lengeler, J. W., Jahreis, K., & Wehmeier, U. F. (1994) *Biochim. Biophys. Acta 1188*, 1−28.

Liao, D. I., Kapadia, G., Reddy, P., Saier, M. H., Reizer, J., & Herzberg, O. (1991) *Biochemistry 30*, 9583−9594.

Lutsenko, S., & Kaplan, J. H. (1995) *Biochemistry 34*, 15608−15613.

Lux, R., Jahreis, K., Bettenbrook, K., Parkinson, J. S., & Lengeler, J. W. (1995) *Proc. Natl. Acad. Sci. U.S.A. 92*, 11583−11587.

Mao, Q., Schunk, T., Flükiger, K., & Erni, B. (1995a) *J. Biol. Chem. 270*, 5258−5265.

Mao, Q., Schunk, T., Gerber, B., & Erni, B. (1995b) *J. Biol. Chem. 270*, 18295−18300.

Marion, D., Kay, L. E., Sparks, S. W., Torchia, D. A., & Bax, A. (1989a) *J. Am. Chem. Soc. 111*, 1515−1517.

Marion, D., Discroll, P. C., Kay, L. E., Wingfield, P. T., Bax, A., Groneborn, A. M., & Clore, M. G. M. (1989b) *Biochemistry 28*, 6150−6156.

Meadow, N. D., Fox, D. K., & Roseman, S. (1990) *Annu. Rev. Biochem. 59*, 497−542.

Meins, M., Jenö, P., Müller, D., Richter, W. J., Rosenbusch, J. P., & Erni, B. (1993) *J. Biol. Chem. 268*, 11604−11609.

Misset, O., Blaauw, M., Postma, P. W., & Robillard, G. T. (1983) *Biochemistry 22*, 6163−6170.

Nuoffer, C., Zanolari, B., & Erni, B. (1988) *J. Biol. Chem. 263*, 6647−6655.

Pas, H. H., Meyer, G. H., Kruizinga, W. H., Tamminga, K. S., van Weeghel, R. P., & Robillard, G. T. (1991) *J. Biol. Chem. 266*, 6690−6692.

Pelton, J. G., Torchia, D. A., Meadow, N. D., Wong, C. Y., & Roseman, S. (1991a) *Proc. Natl. Acad. Sci. U.S.A. 88*, 3479−3483.

Pelton, J. G., Torchia, D. A., Meadow, N. D., Wong, C. Y., & Roseman, S. (1991b) *Biochemistry 30*, 10043−10057.

Pelton, J. G., Torchia, D. A., Meadow, N. D., & Roseman, S. (1992) *Biochemistry 31*, 5215−5224.

Pelton, J. G., Torchia, D. A., Meadow, N. D., & Roseman, S. (1993) *Protein Sci. 2*, 543−558.

Postma, P. W., Lengeler, J. W., & Jacobson, G. R. (1993) *Microbiol. Rev. 57*, 543−594.

Rajagopal, P., Waygood, E. B., & Klevit, R. E. (1994) *Biochemistry 33*, 15271−15282.

Robillard, G. T., Boer, H., van Weeghel, R. P., Wolters, G., & Dijkstra, A. (1993) *Biochemistry 32*, 9553−9562.

Saier, M. H. (1989) *Microbiol. Rev. 53*, 109−120.

Saier, M. H., Cox, D. F., Feucht, B. U., & Novotny, M. J. (1982) *J. Cell. Biochem. 18*, 231−238.

Sander, C., & Schneider, R. (1991) *Proteins 9*, 56−68.

Schnetz, K., Sutrina, S. L., Saier, M. H., & Rak, B. (1990) *J. Biol. Chem. 265*, 13464−13471.
Scholte, B. J., Schuitema, A. R., & Postma, P. W. (1982) *J. Bacteriol. 149*, 576−586.
Schunk, T. (1992) Konstruktion von Fusionsproteinen aus Untereinheiten des bakteriellen Phosphotransferase Systems, Ph.D. Thesis, University of Marburg, Marburg, Germany.
Shaka, A. J., Lee, C. J., & Pines, A. (1988) *J. Magn. Reson. 77*, 274−293.
Stuckey, J. A., Schubert, H. L., Fauman, E. B., Zhang, Z.-Y., Dixon, J. E., & Saper, M. A. (1994) *Nature 370*, 571−575.
Su, X. D., Taddei, N., Stefani, M., Ramponi, G., & Nordlund, P. (1994) *Nature 370*, 575−578.
Takahashi, H., Odaka, A., Kawaminami, S., Matsunaga, C., Kato, K., Shimada, I., & Arata, Y. (1991) *Biochemistry 30*, 6611−6619.
van Nuland, N. A. J., Kroon, G. J. A., Dijkstra, K., Wolters, G. K., Scheek, R. M., & Robillard, G. T. (1993) *FEBS Lett. 315*, 11−15.
van Nuland, N. A. J., Hangyi, I. W., van Schaik, R. C., Berendsen, H. J. C., van Gunsteren, W. F. G., Scheek, R. M., & Robillard, G. T. (1994) *J. Mol. Biol. 237*, 544−559.
van Nuland, N. A. J., Boelens, R., Scheek, R. M., & Robillard, G. T. (1995*) J. Mol. Biol. 246* (1), 180−193.
van Nuland, N. A. J., Wiersma, J. A., Vanderspoel, D., Degroot, B. L., Scheek, R. M., & Robillard, G. T. (1996) *Protein Sci. 5* (3), 442−446.
Vogler, A. P., Broekhuizen, C. P., Schuitema, A., Lengeler, J. W., & Postma, P. W. (1988*) Mol. Microbiol. 2*, 719−726.
Wittekind, M., Reizer, J., Deutscher, J., Saier, M. H., Jr., & Klevit, R. E. (1990*) Biochemistry 29*, 7191−7200.
Worthylake, D., Meadow, N. D., Roseman, S., Liao, D.-I., Herzberg, O., & Remington, S. J. (1991) *Proc. Natl. Acad. Sci. U.S.A. 88*, 10382−10386.
Zhou, H., Lowry, D. F., Swanson, R. V., Simon, M. I., & Dahlquist, F. W. (1995*) Biochemistry 34*, 13858−13870.

BI963053V